Finite Capacitive Response at the Quantum Hall Plateau

Lili Zhao(赵利利)[1], Wenlu Lin(林文璐)[1], Y. J. Chung[2], K. W. Baldwin[2], L. N. Pfeiffer[2], and Yang Liu(刘阳)[1*]

[1]*International Center for Quantum Materials, Peking University, Beijing 100871, China*
[2]*Department of Electrical Engineering, Princeton University, Princeton, New Jersey 08544, USA*

(Received 11 May 2022; accepted manuscript online 1 August 2022)

We study ultra-high-mobility two-dimensional (2D) electron/hole systems with high precision capacitance measurement. It is found that the capacitance charge appears only at the fringe of the gate at high magnetic field when the 2D conductivity decreases significantly. At integer quantum Hall effects, the capacitance vanishes and forms a plateau at high temperatures $T \gtrsim 300\,\mathrm{mK}$, which surprisingly disappears at $T \lesssim 100\,\mathrm{mK}$. This anomalous behavior is likely a manifestation that dilute particles/vacancies in the top-most Landau level form Wigner crystals, which have finite compressibility and can host polarization current.

DOI: 10.1088/0256-307X/39/9/097301

A strong perpendicular magnetic field B quantizes kinetic energy of electrons/holes into a set of discrete Landau levels. The discrete level structure gives rise to formation of incompressible quantum Hall liquids, an insulating phase with vanishing longitudinal conductance and quantized Hall conductance.[1–3] Another insulating phase appears when the Landau level filling factor $\nu = nh/eB$ is small,[4,5] which is generally believed to be a Wigner crystal pinned by a small but ubiquitous disorder potential.[6] In state-of-the-art high-mobility 2D systems, Wigner crystals are also seen near integer $\nu = N$ (N is a positive integer) when the particles/vacancies in the topmost Landau level have sufficiently low effective filling factors $\nu^* = |\nu - N|$.[7–10]

Capacitance is of great interest in quantum measurements.[11–25] The chemical potential μ of a Fermion system depends on its particle density, leading to the quantum capacitance that is proportional to the density of states at the Fermi energy. High sensitivity capacitance measurements can reveal fine structures of the systems' energy levels, such as the formation of delicate quantum phases,[14–19] the non-parabolic dispersion,[20] the interaction induced negative compressibility,[21,22] the minibands and Fermi contour transitions in multi-band 2D materials.[23–25] Unfortunately, quantitative studies using high precision capacitive measurement at mK-temperature are limited.

In this Letter, we report our high-precision capacitance studies on ultra-high-mobility 2D electron/hole systems at mK-temperature. We find that the device capacitance C has a strong positive dependence on the 2D longitudinal sheet conductance σ. Our observation suggests that the capacitance charge appears only at the fringe of the gate. C at integer Landau level filling factor ν approaches zero, agrees with the expectation that the zero σ prohibits charge being transported. In the vicinity of integer ν, the C plateau is seen as wide as the σ plateau at $T \simeq 300\,\mathrm{mK}$. Surprisingly, it disappears at lower temperatures while the σ plateau becomes even wider. This anomalous behavior is likely induced by the Wigner crystal formed by the dilute particles/vacancies in the topmost Landau level.

The samples used in this study are made from GaAs wafers grown by molecular beam epitaxy along the (001) direction. These wafers consist of GaAs quantum well bounded on either side symmetrically by undoped AlGaAs spacer layers and δ-doping layers. Samples A, B and D are Si-doped electron systems with 30-nm-wide quantum well, as-grown density $n \simeq 2.0 \times 10^{11}\,\mathrm{cm}^{-2}$ and mobility $13 \times 10^6\,\mathrm{cm}^2/(\mathrm{V{\cdot}s})$. Sample C is C-doped hole system with 17.5-nm-wide quantum well, as-grown density $p \simeq 1.6{\times}10^{11}\,\mathrm{cm}^{-2}$ and mobility $1.6{\times}10^6\,\mathrm{cm}^2/(\mathrm{V{\cdot}s})$. Each sample has alloyed InSn or InZn contacts at the four corners of a $2 \times 2\,\mathrm{mm}^2$ piece cleaved from the wafer. For each sample, we evaporate several separate Au/Ti front gates with different geometries, and measure the gate-to-gate capacitance. Samples A and B consist 500 μm-separated square gates with side length $l = 200$ and 100 μm, respectively [Fig. 1(b)]. Samples C and D consist concentric gates [Fig. 3(b) inset]. The inner gate radius of sample C/D is 75/60 μm, and the gap between the two gates is 75/60 μm. We have compared the samples with different gate geometries, and find that the observed features have no substantial dependence on the gate geometry (data not shown). The measurements are carried out in a dilution refrigerator with base temperature $T \simeq 30\,\mathrm{mK}$.

Figure 1 depicts the principle of our measurement.[26] The passive bridge installed at the sample stage consists of one resistance arm and one capacitance arm. The resistance arm includes a reference resistance R_r and one voltage-controlled-variable-resistance R_h, implemented by the source-to-drain resistance of a high-electron-mobility transistor. We tune R_h via the transistor's gate voltage V_h, and measure R_h and R_r *in situ* with a low-frequency lock-in technique. We excite the bridge with a radio-frequency voltage (typically $\simeq$130 MHz, $\simeq$0.5 $\mathrm{mV_{PP}}$) differentially coupled between V_in^+ and V_in^-. We amplify the bridge output V_out and measure its amplitude and phase with a custom-built radio-frequency lock-in amplifier. The

*Corresponding author. Email: liuyang02@pku.edu.cn
© 2022 Chinese Physical Society and IOP Publishing Ltd

measured $|V_{\rm out}|$ reaches minimum value V_0 when the bridge is balanced, e.g., $R_{\rm h}/R_{\rm r} = C/C_{\rm r}$, see Fig. 1(b). By properly choosing the reference phase, we can separate $V_{\rm out}$ into the in-phase and out-of-phase components V_X and V_Y. $V_X = 0$ when the bridge is balanced and has a linear dependence on $\kappa = R_{\rm h}/(R_{\rm h}+R_{\rm r})$ with slope $S = \partial V_X/\partial\kappa$, see Fig. 1(c). $V_Y \simeq V_0$ is nearly independent of κ. In the vicinity of the balance point, we can also deduce the C from the approximation $V_X = -S\cdot(\frac{C}{C+C_{\rm r}} - \kappa)$, which agrees with the value measured by balancing the bridge, see Fig. 2(b).

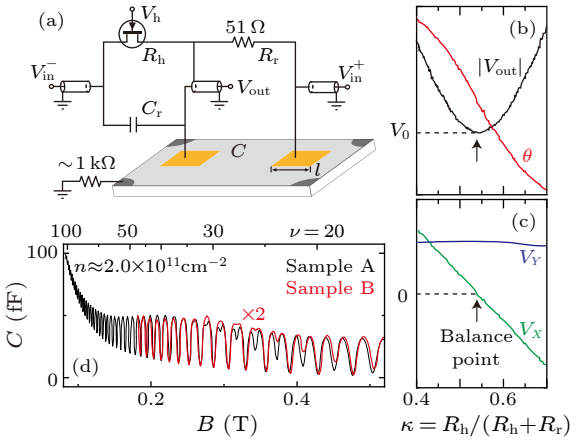

Fig. 1. (a) Circuit diagram of our capacitance measurement setup. The device is the capacitance between two gates (yellow square). The contacts (dark gray) are connected to ground with a resistor. The grounding of contacts does not cause any change in the result. (b) The measured amplitude and phase of output signal. $|V_{\rm out}|$ reaches its minimum V_0 and $\theta = -\pi/2$ when the bridge is at balance point, indicated by the black arrows. (c) $V_{\rm out}$ can be separated into the in-phase and out-of-phase components, $V_X = |V_{\rm out}|\cdot\cos\theta$ and $V_Y = |V_{\rm out}|\cdot\sin\theta$. (d) The C vs B taken from samples A (black) and B (red). The red trace is amplified by a factor of 2. The temperature is 30 mK.

The C data in Fig. 1(d) appreciates the merit of our high precision measurement. As B increases, C decreases dramatically from its $B = 0$ value (which is close to the estimated geometric capacitance of a few pF) by orders of magnitude.[27] The similar phenomenon has been reported in previous experiments where the screening capability of high quality 2D reduces significantly at high field.[22] The shrinking of C is less violent in samples which have shorter scattering time or smaller size, or when we use lower measurement frequencies, also consistent with other studies.[13,14,16] In Fig. 1(d), we compare data taken from samples A and B, whose gate dimensions differ by a factor of 2 and center-to-center distances are kept the same. In both samples, the capacitance oscillation starts at $B \lesssim 0.01$ T when $\nu \gtrsim 150$, evidencing that our measurement is as gentle as DC transport. Interestingly, the traces taken from two samples are nearly a replica of each other but scales by a factor of 2.

We can understand these features with the model shown in Fig. 2(a). The 2D system is grounded through contacts remote from the gates. A time-varying voltage $V\cdot e^{i\omega t}$ applied on the gate induces an oscillating capacitance charge density $Q(\boldsymbol{r})\cdot e^{i\omega t}$ in the 2D system satisfying $Q(\boldsymbol{r}) = \frac{\varepsilon}{d}(V - \mu(\boldsymbol{r})/q)$, where ε is the dielectric constant, d is the gate-to-2D distance, $q = \pm e$ is the particle's charge, and $\mu(\boldsymbol{r})$ is the local chemical potential of the 2D system. For simplicity, we neglect the time-dependence term $e^{i\omega t}$ and replace $\partial/\partial t$ with $i\omega$ in the following. The spatial variation of $\mu(\boldsymbol{r})$ generates a current distribution $\boldsymbol{j}(\boldsymbol{r}) = \frac{\sigma}{q}\nabla\mu(\boldsymbol{r})$ in the 2D system and by the charge conservation law, $\nabla\cdot\boldsymbol{j}(\boldsymbol{r}) = i\omega\cdot Q(\boldsymbol{r})$.

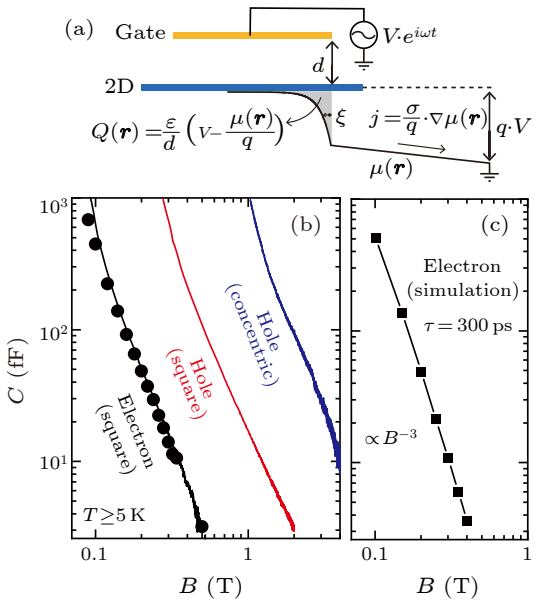

Fig. 2. (a) The model describing the capacitance response of our device. The AC voltage $V_0\cdot e^{i\omega t}$ applied to the gate varies the chemical potential $\mu(\boldsymbol{r})$ of the underlying 2D system, inducing a capacitance charge density $Q(\boldsymbol{r})$ and the corresponding current density $\boldsymbol{j}(\boldsymbol{r})$. (b) C measured from three different samples at high temperatures $T \geq 5$ K. The symbols represent C deduced from the balance condition and the lines are the results converted from V_X. (c) Numerical simulation predicts the $C \propto B^{-3}$ dependence. We use $\tau = 300$ ps to match with Fig. 2(b) electron data.

At high field when $\omega_{\rm C}\tau \gg 1$, $\omega_{\rm C}$ is the particles' cyclotron frequency and τ is their scattering time, the σ of an ultra-high mobility 2D system vanishes as $\sigma \simeq \sigma_{(B=0)}/(1+(\omega_{\rm C}\tau)^2)$. $\nabla\mu(\boldsymbol{r})$ is almost zero except at the proximity of the gate boundary, and $\mu(\boldsymbol{r}) \approx qV$ at the center of the gate. Near this edge, $Q(\boldsymbol{r}) \propto \pm\exp(-|x|/\xi)$ and $\xi = \sqrt{\sigma d/(\omega\varepsilon)}$, where x is the distance from the boundary. Furthermore, the current induced potential change outside the gated region as well as the parasitic capacitance $C_{\rm P}$ becomes non-negligible when σ is small. Combining all the above-mentioned effects, the $C = \int Q(\boldsymbol{r})d\boldsymbol{r}/V$ is proportional to the length of the gate perimeter and reduces as B^{-3}, see the numerical results in Fig. 2(c). We show C measured in 2D electron and hole samples with different gate geometries in Fig. 2(b). The measured C is in nearly perfect agreement with the B^{-3} prediction. This model also predicts that C decreases slower if τ is smaller or the effective mass is larger, also consistent with our observation in Fig. 2(b), where C in 2D hole systems is usually higher than in 2D electron systems at high field.

Based on the model shown Fig. 2, the out-of-phase signal V_Y is a good measure of conductance, $G \propto \sigma$, where $V_Y = V_0 - S \cdot (\frac{G}{G+\omega C_r} - \kappa)$ if $\omega_C \tau \gg 1$. Figure 3(a) shows the deduced G and the R_{xx} of sample A obtained from the *in situ* quasi-DC transport measurement using the four corner contacts. Both G and R_{xx} traces have wide, flat plateaus when the 2D system forms incompressible integer quantum Hall insulator at $\nu = 1, 2, 3, \ldots$ We also notice that C and G are remarkably similar with each other. This may not be surprising since the model in Fig. 2 predicts that C strongly entangles with G. Mysteriously, no plateau is seen in the C trace at integer fillings while one would expect vanishing C when $G = 0$. The missing plateau in C is substantiated by data shown in Fig. 3(b), taken from sample C which is a 2D hole system with concentric gate geometry.

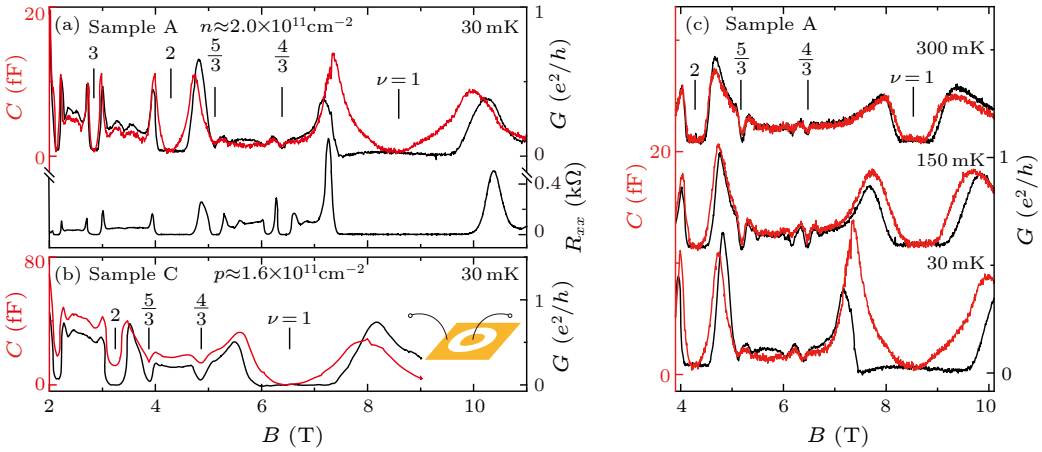

Fig. 3. (a) C, G, and R_{xx} taken from electron sample A. (b) C and G taken from hole sample C. (c) C and G taken from sample A at different temperatures. Traces are offset vertically. The excitation frequency of (a)–(c) is ≃ 130 MHz.

In Fig. 3(c), the data taken from sample A at 30, 150 and 300 mK is even more intriguing. At the highest temperature $T \simeq 300$ mK, the C and G traces are almost exact replica of each other. Both of them have well-developed plateau at $\nu = 1$ and 2, a manifestation that the 2D system forms quantum Hall insulator and the extra particles/holes in the vicinity of $\nu = 1$ and 2 are localized and cannot response to external electric field. When the 2D system becomes colder, the C remains zero at exact integer fillings $\nu = 1$ and 2, but its plateau gradually becomes narrower and eventually disappears at $T \simeq 30$ mK while the G plateau broadens.

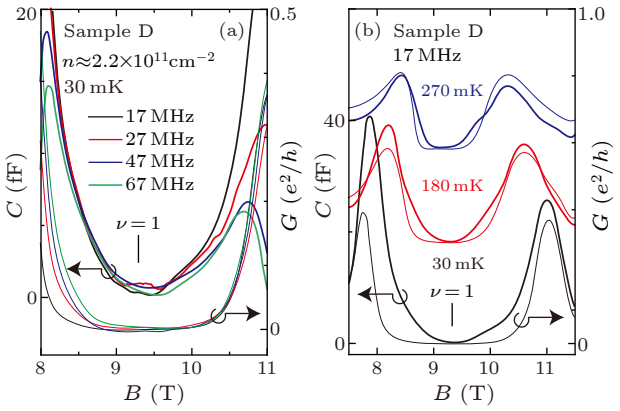

Fig. 4. C (thick line) and G (thin line) taken from sample D near $\nu = 1$. (a) Measurements at different frequencies. The temperature is 30 mK. (b) Measurements at different temperatures. The excitation frequency is ≃ 17 MHz. Traces are offset vertically.

At $T \simeq 30$ mK, the C values of sample D measured at different frequencies are nearly the same within the $\nu = 1$ integer quantum Hall plateau, see Fig. 4(a). The temperature dependence of 17-MHz data in Fig. 4(b) resembles the result in Fig. 3(c). Therefore, the non-vanishing C phenomenon is independent of gate geometries, carrier types and measurement frequencies.

The fact that C becomes finite at low temperatures while $G = 0$ suggests that charge can still be effectively transported in-plane while the 2D system is not conducting. Plateaus appear near $\nu = 1$ and 2 in the high-temperature trace when the system exhibits incompressible quantum Hall insulators, because the extra particles/vacancies are localized and cannot response to the AC voltage. Surprisingly, C becomes finite at low temperature when the localization is expected to be stronger. However, in samples with mobility ∼2 × 10^4 cm^2/(V·s) where localization is strong, C plateaus at integer fillings are clearly seen till 30 mK (data not shown).

One plausible explanation is the existence of a long-range correlated compressible phase which is stable only at low temperatures. It has been suggested by previous studies that the dilute particles/vacancies in the topmost Landau level may form a Wigner crystal in the vicinity of integer filling factors.[7] This solid phase cannot host conducting current, but its deformation in time-varying external electric field generates polarization current. The finite C is an outcome of the finite compressibility of this Wigner crystal. Note that ∼10 fF capacitance in our typical measurements corresponds to relocation of ∼10 electrons/holes per cycle between two gates. Therefore, the measurement-induced deformation is just a perturbation to the Wigner crystal. The frequency we used is well below the Wigner crystal resonant frequency (typically a few GHz) reported

in Ref. [7], which is still on the low-frequency limit. In such a scenario, C approaching zero at $T \gtrsim 200\,\mathrm{mK}$ signalizes the melting of the Wigner crystal.

In conclusion, with the help of our high-precision capacitance measurement setup, we have carefully studied the capacitance response of ultra-high mobility 2D systems at mK temperature. Our result shows that the device capacitance strongly entangles with the 2D conductance G and vanishes if $G = 0$. Surprisingly, at the $G = 0$ plateau of integer quantum Hall effects, C is only zero at high temperatures but becomes finite at base temperature. This anomalous behavior is consistent with the formation of compressible Wigner crystal which can response to AC voltage through polarization current.

This work was supported by the National Natural Science Foundation of China (Grant Nos. 92065104 and 12074010), in part by the Gordon and Betty Moore Foundation's EPiQS Initiative (Grant No. GBMF9615) to L. N. Pfeiffer, and by the National Science Foundation MRSEC (Grant No. DMR 2011750) to Princeton University. We thank M. Shayegan, L. W. Engel, Xin Wan, Bo Yang, and Wei Zhu for valuable discussion.

References

[1] Prange R E and Girvin S M 1987 *The Quantum Hall Effect* (New York: Springer)
[2] Sarma S D and Pinczuk A 1997 *Perspectives in Quantum Hall Effects* (New York: Wiley)
[3] Jain J K 2007 *Composite Fermions* (Cambridge: Cambridge University Press)
[4] Jiang H W, Willett R L, Stormer H L, Tsui D C, Pfeiffer L N, and West K W 1990 *Phys. Rev. Lett.* **65** 633
[5] Goldman V J, Santos M, Shayegan M, and Cunningham J E 1990 *Phys. Rev. Lett.* **65** 2189
[6] See articles by Fertig H A and by Shayegan M in Ref.[2].
[7] Chen Y, Lewis R M, Engel L W, Tsui D C, Ye P D, Pfeiffer L N, and West K W 2003 *Phys. Rev. Lett.* **91** 016801
[8] Liu Y, Pappas C G, Shayegan M, Pfeiffer L N, West K W, and Baldwin K W 2012 *Phys. Rev. Lett.* **109** 036801
[9] Hatke A T, Liu Y, Magill B A, Moon B H, Engel L W, Shayegan M, Pfeiffer L N, West K W, and Baldwin K W 2014 *Nat. Commun.* **5** 4154
[10] Myers S A, Huang H, Pfeiffer L N, West K W, and Csáthy G A 2021 *Phys. Rev. B* **104** 045311
[11] Kaplit M and Zemel J N 1968 *Phys. Rev. Lett.* **21** 212
[12] Voshchenkov A M and Zemel J N 1974 *Phys. Rev. B* **9** 4410
[13] Smith T P, Goldberg B B, Stiles P J, and Heiblum M 1985 *Phys. Rev. B* **32** 2696
[14] Mosser V, Weiss D, Klitzing K, Ploog K, and Weimann G 1986 *Solid State Commun.* **58** 5
[15] Ashoori R C, Stormer H L, Weiner J S, Pfeiffer L N, Pearton S J, Baldwin K W, and West K W 1992 *Phys. Rev. Lett.* **68** 3088
[16] Smith T P, Wang W I, and Stiles P J 1986 *Phys. Rev. B* **34** 2995
[17] Yang M J, Yang C H, Bennett B R, and Shanabrook B V 1997 *Phys. Rev. Lett.* **78** 4613
[18] Eisenstein J P, Pfeiffer L N, and West K W 1994 *Phys. Rev. B* **50** 1760
[19] Zibrov A A, Kometter C, Zhou H, Spanton E M, Taniguchi T, Watanabe K, Zaletel M P, and Young A F 2017 *Nature* **549** 360
[20] Irie H, Akiho T, and Muraki K 2019 *Appl. Phys. Express* **12** 063004
[21] Eisenstein J P, Pfeiffer L N, and West K W 1992 *Phys. Rev. Lett.* **68** 674
[22] Deng H, Pfeiffer L N, West K W, Baldwin K W, Engel L W, and Shayegan M 2019 *Phys. Rev. Lett.* **122** 116601
[23] Jo J, Garcia E A, Abkemeier K M, Santos M B, and Shayegan M 1993 *Phys. Rev. B* **47** 4056
[24] Zibrov A A, Rao P, Kometter C, Spanton E M, Li J I A, Dean C R, Taniguchi T, Watanabe K, Serbyn M, and Young A F 2018 *Phys. Rev. Lett.* **121** 167601
[25] Tomarken S L, Cao Y, Demir A, Watanabe K, Taniguchi T, Jarillo-Herrero P, and Ashoori R C 2019 *Phys. Rev. Lett.* **123** 046601
[26] Zhao L, Lin W, Fan X, Song Y, Lu H, and Liu Y 2022 *Rev. Sci. Instrum.* **93** 053910
[27] In samples A, B and C, our measured capacitance approaches a constant value $\simeq$60 fF when the particles form incompressible integer quantum Hall liquid. This is likely the parasitic capacitance C_P induced by the bonding wires, gates, etc. In sample D, C_P is reduced to $\simeq$15 fF because we add one impedance matching network at the input of the bridge at the sample stage. We have subtracted C_P in all figures.